Scenario-based approaches for handling uncertainty in MPC for power system frequency control ⋆

Anne Mai Ersdal [*,**] **Lars Imsland** [**]

[*] *Department of Engineering Science and Safety IVT*
UiT The Arctic University of Norway, Tromsø, Norway
(e-mail: {anne.mai.ersdal}@uit.no).
[**] *Department of Engineering Cybernetics*
Norwegian University of Science and Technology, Trondheim, Norway
(e-mail: {anne.mai.ersdal,lars.imsland}@ntnu.no).

Abstract: A stochastic nonlinear model predictive controller (SNMPC) is designed for automatic generator control of a proxy of the Nordic power system, and it is compared with a multi-stage nonlinear model predictive controller (MNMPC). Both controllers are scenario based, but originate in two different disturbance modeling paradigms; stochastic and deterministic. A simulation study indicates that the two controllers behave similarly. The MNMPC is however less exposed to infeasibility issues, and it also has better tractability than the SNMPC. On the other hand, the SNMPC gives probabilistic guarantees for constraint fulfillment; a feature whose practical implications are debatable.

Keywords: Optimal operation and control of power systems, Control system design.

1. INTRODUCTION

Model predictive control (MPC) is a framework for advanced control that has its roots in optimal control, and it is one of the few advanced control methods that has made a significant impact on industrial control engineering (Maciejowski, 2002). In short, the MPC solves a finite-horizon optimal control problem (OCP) at each time step and then implements the first instant of the solution in a receding horizon manner.

The MPC relies on good knowledge of the system it is controlling, and the system model is very important. Full knowledge and 100% accurate models are however extremely rare, and in practice the MPC must be able to account for uncertainties and/or unmeasurable disturbances acting on the system. One way to systematically address this issue is through robust MPC (RMPC), which considers uncertainties that are assumed to be deterministic and lie in a bounded set (Mesbah, 2016; Bemporad and Morari, 1999). The work on RMPC has been dominated by min-max OCP formulations (Bemporad et al., 2003; Scokaert and Mayne, 1998), and relaxations such as tube-based MPC (Langson et al., 2004). The RMPC is designed so that system constraints are fulfilled for all possible disturbances within the prediction horizon, which often can lead to conservative results. A practical approach to achieve robust MPC which is not as conservative, is multi-stage MPC. The multi-stage MPC is based on a representation of the evolution of the uncertainty as a scenario tree (Lucia et al., 2013), where the uncertainty is assumed to be discrete. The concept of future feedback is also included by allowing different inputs for different disturbance scenarios, reducing the conservativeness of the robust approach (Lucia et al., 2013). Allowing feedback in the MPC predictions results in what is often referred to as feedback MPC Rawlings and Mayne (2009), and in the presence of uncertainty feedback MPC is known to be superior to nominal MPC, though resulting in a more complex OCP (Rawlings and Mayne, 2009). An alternative approach to implementing feedback MPC is optimizing over control laws $u = \mu(x)$, rather than control actions (Rawlings and Mayne, 2009). This is used in e.g. tube-base MPC. For the general nonlinear case, there are no guarantees that the multi-stage MPC results in robust constraints satisfaction for scenarios that are not included in the scenario tree, but it has been shown to give good results in practice (Lucia et al., 2013, 2014b).

An alternative to RMPC is stochastic MPC (SMPC), where the uncertainties are considered to be of probabilistic nature. The probabilistic description of uncertainties are used to define chance constraints (Li et al., 2002; Primbs and Sung, 2009) which enable systematic use of the stochastic description of uncertainties to define stochastic levels of acceptable closed-loop constraint violation (Mesbah, 2016), i.e. a small constraint violation probability is allowed. Chance-constrained optimization problems are hard to solve in general, and sample-based approximations such as the scenario approach (Campi et al., 2009) have been presented as tractable alternatives. In the scenario approach only a finite number of uncertainty realizations are considered, and the chance-constraint optimization problem is approximated by replacing the chance con-

⋆ The financial support from the Research Council of Norway project 207690 "'Optimal Power Network Design and Operation"' is gratefully acknowledged.

Δf	Frequency
ΔP_m	Produced power
ΔP_D	Unpredicted power imbalance
ΔP_{tie}	Total power flow from the area to all other areas
H	Inertia of the rotating masses
T_{ij}	Synchronizing torque coefficient between area i and j
Δc	Change in valve opening from c_{ss}
Δq	Change in water flow rate from q_{ss}
T_w	Water starting time of the hydro turbine
A_t	Factor that accounts for the different per-unit bases in the turbine and generator
$\Delta\xi_2$	Integral of the governor
$\Delta\xi_3$	Valve opening of the main servo motor of the governor
T_g	Time constant of the servo motor
T_r	Time constant of the transient droop
r	Transient-droop coefficient
ρ	Constant-droop coefficient
Δc	Saturated valve opening
Δc_r	Reference point for valve opening
Δc^i_{rj}	Reference point for valve opening in generator j in area i
α^i_j	Participation factor for generator j in area i

Table 1. Definitions of symbols in Equation (1). All variables are deviations from a given operating point.

straint with hard constraints associated with the extracted disturbance realizations only.

This work compares the performance of a stochastic nonlinear MPC (SNMPC) inspired by Campi et al. (2009) and a multi-stage nonlinear MPC (MNMPC) similar to the robustified NMPC in Ersdal et al. (2016b), for automatic generator control (AGC) of the Nordic power system. AGC is currently facing challenges related to stability and reliability due to more intermittent energy resources in the system as well as an increasing power demand, and during the last decade there has been an increasing interest in applying MPC for AGC, see for example Venkat et al. (2008); Shiroei et al. (2013); Ersdal et al. (2016a,b). SMPC has also been investigated as a method for reserve scheduling for power systems with wind power generation (Rostampour et al., 2013). In this work, the uncertainty of the model is dominated by the fluctuations in produced wind power, and the aim is to design an NMPC for AGC which is robust against these fluctuations.

The remainder of this paper is organized as follows. In Section 2 the system model is presented before the SNMPC and the MNMPC are discussed in Section 3. In Section 4, the details of the case study are given and the results from simulations on the proxy model are presented. The concluding remarks are summarized in Section 5.

2. MODEL DESCRIPTION

In large, complex power systems, such as the Nordic power system, one important control aspect is frequency control (FC). This is a term applied to describe the continuous operation of keeping the frequency of a power system stable, which is strongly connected to the balancing of produced and consumed power. It is vital for the power system that this power balance is maintained and that the produced power matches the consumed power at all times, if not the generators could loose synchronism and the power system would collapse.

AGC is the part of FC that automatically controls the generator production set points, and in Ersdal et al. (2016a) an NMPC is designed for AGC of the Nordic power system. This is extended in Ersdal et al. (2016b) to a robustified NMPC which is designed to be more robust against fluctuations in produced wind power, by including worst-case scenarios of these. In Ersdal et al. (2016a,b) the NMPC is based on a simplified model, while tested on a more rigorous and realistic proxy model. In this work, the same models will be used, however, only the equations for the NMPC prediction model (PM) are repeated here. The interested reader is referred to Ersdal et al. (2016b) for details of the SINTEF model, which is used as a proxy for the physical system.

In the Nordic power system the hydro turbines account for nearly 100% of the AGC, and so only the hydro turbine dynamics are included in the model. Other turbines are included as constant power inputs. The PM is divided into N areas, and the equations for each area i are as follows

$$\Delta\dot{f}^i = \frac{1}{2H^i}\left(\Delta P^i_m - \Delta P^i_D - \Delta P^i_{tie}\right) \tag{1a}$$

$$\Delta\dot{q}^i = -\frac{2}{T^i_w c^{i2}_{ss}/q^i_{ss}}\left(\Delta q^i - \frac{q^{i2}_{ss}}{c^{i2}_{ss}}\Delta c^i\right) \tag{1b}$$

$$\Delta\dot{\xi}^i_2 = -\frac{1}{T^i_r}\Delta\xi^i_2 + \Delta c^i \tag{1c}$$

$$\Delta\dot{\xi}^i_3 = \mathrm{sat}^i_{\dot{c}}\left(\frac{\Delta c^i_r - \Delta f^i + \frac{r^i}{T^i_r}\Delta\xi^i_2 - \left(r^i+\rho^i\right)\Delta c^i}{T^i_g}\right) \tag{1d}$$

$$\Delta\dot{P}^i_{tie} = 2\pi\left(\Delta f^i \sum_{j=1,j\neq i}^{N} T_{ij} - \sum_{j=1,j\neq i}^{N} T_{ij}\Delta f^j\right) \tag{1e}$$

where

$$\Delta P^i_m = A^i_t\frac{q^{i2}_{ss}}{c^{i2}_{ss}}\left(3\Delta q^i - 2\frac{q^{i2}_{ss}}{c^{i2}_{ss}}\Delta c^i\right) \tag{1f}$$

$$\Delta c^i = \mathrm{sat}^i_c\left(\Delta\xi^i_3\right) \tag{1g}$$

$$\Delta c^i_{rj} = \alpha^i_j\Delta c^i_r \tag{1h}$$

where $i = 1,\cdots,N$, and the variables and parameters are explained in Table 1. The controllable input to the system is the valve-opening setpoint for each area Δc^i_r and the participation factor for each generator j in area i; α^i_j. The disturbance acting on the system is the unpredicted power imbalance for each area ΔP^i_D.

2.1 System disturbance

The only disturbance we consider is that of the unpredicted power imbalance ΔP^i_D. The main components of the unpredicted power imbalance with regards to FC is the imbalance in production and consumption from intermittent generators and loads, respectively. When dealing with power systems including a certain amount of wind power, such as the Nordic system, one can for simplicity assume that ΔP^i_D is dominated by the fluctuations in produced wind power. If, in addition, it is assumed that the majority of wind power is situated in area p, ΔP_D of all the other areas can be neglected, and the model is affected by one single disturbance $\Delta P_D = \Delta P^p_D$. With the Nordic network in mind, Denmark and South Sweden contribute with

about 80% of the total wind power production (Statnett, 2012).

The complete model is thus given by the nonlinear model

$$\dot{x} = f(x, u, w) \tag{2}$$

where $x = \left[\Delta f^i \ \Delta q^i \ \Delta \xi_2^i \ \Delta \xi_3^i \ \Delta P_{tie}^i\right]$, $u = \left[\Delta c_r^i \ \alpha_j^i\right]$, $w = \Delta P_D$, $i = 1, \cdots, N$, $j = 1, \cdots, m_h^i$, and m_h^i is the number of hydro generators in area i. The system is also subjected to both input and state constraints

$$g(x, u) \leq 0 \tag{3}$$

including generation constraints, generator rate constraints, and constraints on the tie-line power transfer.

3. CONTROLLER

3.1 Disturbance modeling, deterministic vs stochastic.

When modeling a disturbance influence on a system, it is common to differentiate between deterministic and stochastic modeling. A system disturbance w is in general defined by an admissible set of disturbance signals $w \in \mathcal{W}$, and the difference between deterministic and stochastic modeling is whether or not one attempts to assign probabilities to the elements of the set $\mathcal{W}$ (Levine, 2010). With a deterministic disturbance model all realizations in $\mathcal{W}$ are bounded and considered equally likely to occur, while they are appointed different probabilities $\mathcal{P}[w]$ and are not necessarily bounded when applying a stochastic disturbance model.

The disturbance acting on the system presented in Section 2 is the unpredicted power imbalance $w = \Delta P_D$, which is assumed to be dominated by fluctuations in produced wind power in area p. For each wind farm in area p, the probability space of the future variation from the predicted power output can be estimated (Holttinen, 2004), and from this one can find the probability space of the future variation from the predicted power output for all wind farms in area p combined, i.e. $w \in \mathcal{W}$, see Fig. 2. The estimate of $\mathcal{W}$ is primarily based on weather prognoses, which are stochastic by nature through the use of ensemble forecasting and model output statistics (Barry and Chorley, 2003). Hence, it would in many ways be natural to assign probabilities to the elements of $\mathcal{W}$. However, it is not necessarily the best choice when taking other aspects into account, and in this paper two scenario-based approaches are compared, the SNMPC that is based on a stochastic disturbance model, and the MNMPC that is based on a deterministic disturbance model. The aim of this paper is to compare the two approaches, and discuss their strengths and weaknesses in view of their performance in the case study.

3.2 Stochastic NMPC

Given a system such as (2), if the disturbance signal w is modeled as a stochastic disturbance with probability space $\mathcal{W}$ and probability distribution $\mathcal{P}[w]$ over $\mathcal{W}$, then it makes sense to replace hard constraints with chance constraints

$$\mathcal{P}_w\left[g(x, u) \leq 0 \ \forall \ t\right] \geq 1 - \sigma \tag{4}$$

where $\sigma \in (0, 1)$ is the admissible constraint violation parameter, $t = 1, \cdots, T$, T is the optimization horizon, and $\mathcal{P}_w$ denotes the dependency of $g(x, u)$ on the stochastic signal w. It basically states that the constraints are allowed to be violated with a probability no higher than $1 - \sigma$.

In scenario-based approaches to stochastic NMPC (Campi et al., 2009), S independent identically distributed samples of w $(w^1, \cdots, w^S)$ are used to approximate the chance constraint, where only the constraints corresponding to the extracted disturbance realizations are considered. The result is the SNMPC which includes a standard OCP with a finite number of constraints

$$\min_u \sum_{j=1}^{S} J\left(x^j, u\right) \tag{5a}$$

$$\dot{x}^j - f\left(x^j, u, w^j\right) = 0 \ \text{ System model} \tag{5b}$$

$$g\left(x^j, u\right) \leq 0 \ \text{ Constraints} \tag{5c}$$

where $j = 1, \ldots, S$, x^j and w^j are the state and disturbance associated with scenario j, u the input, and $J(x^j, u)$ the following objective function.

$$J\left(x^j, u\right) = \int_{t=0}^{T} x^{jT} Q^j x^j + u^T R u \ dt \tag{6}$$

For convex OCPs, the scenario approach can be used to find the number of scenarios needed to guarantee that the optimal solution to (5), u^*, satisfies all constraints except a user-chosen fraction that tends rapidly to zero as S increases (Campi et al., 2009). The OCP (5) in the SNMPC has a quadratic objective function and linear state and input constraints. The constraints imposed by the system model (5b) are however nonlinear because of the saturations in (1), hence the OCP is non-convex. It can however be argued that this is a modest nonlinearity, and we will apply the theory in Campi et al. (2009) as if we have a linear model and hence a convex OCP.

Generating scenarios The scenarios used in the SNMPC are found by applying random numbers to generate S independent and identically distributed disturbance realizations $w^j(t) = \Delta P_D^j(t)$, $j = 1, \ldots, S$, $t = 0, \ldots, T$ using the method in Cecílio et al. (2013) with the probability space $\mathcal{W}$ as input. This method results in an unknown probability distribution $\mathcal{P}$, however, using the method of Campi et al. (2009) there is no need to know $\mathcal{W}$ or $\mathcal{P}$ explicitly, only S realizations fulfilling this probability distribution are needed. When selecting the number of scenarios S, Theorem 1 in Campi et al. (2009) states that given the number of optimization variables n_u, if S fulfills

$$S \geq \frac{2}{\epsilon}\left(\ln\frac{1}{\beta} + n_u\right) \tag{7}$$

the resulting solution to (5), u^*, will satisfy the chance constraints (4) with a probability no smaller than $1 - \beta$, except for at most an ϵ-fraction. Theorem 1 in Campi et al. (2009) is developed with one common input u for all scenarios, and so u is equal for all j in the SNMPC (5).

3.3 Multi-stage NMPC

In Ersdal et al. (2016b) an NMPC for AGC of the Nordic power system which is robustified against fluctuations in produced wind power is presented. It is a special case of the multi-stage NMPC (MNMPC) presented in Lucia et al. (2013), and it is also inspired by the min-max feedback MPC presented in Scokaert and Mayne (1998). In both

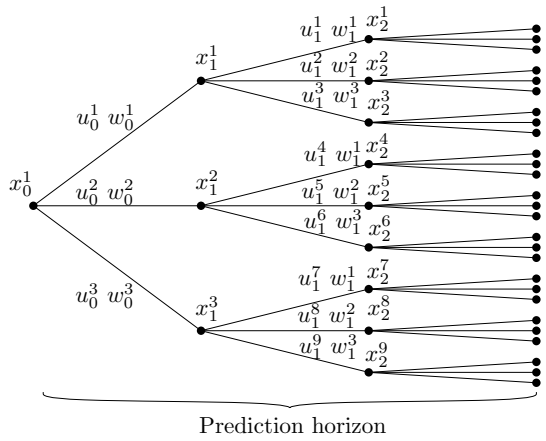

Fig. 1. Scenario tree representation of the discrete uncertainty evolution for multi-stage NMPC (Lucia et al., 2013).

Lucia et al. (2013) and Scokaert and Mayne (1998) the concept of future feedback is included in the MPC. The idea is that the future control inputs can be adapted to the future disturbance measurements/estimates, and that only decisions based on the same information must be equal (Lucia et al., 2013). A scenario tree is presented in Lucia et al. (2013), where the uncertainty is represented by discrete scenarios and the branches are combinations of values from the assumed extreme values of the disturbance, see Fig. 1. If future feedback is not included, as is the case with the SNMPC, the input u would have to be equal for all disturbances and state evolutions in the scenario-tree. With a discrete disturbance representation, as depicted in Fig. 1, this means that

$$u_0^1 = u_0^2 = u_0^3, \;\; u_1^1 = u_1^2 = \cdots = u_1^9.$$

With the MNMPC, however, only the inputs originating in the same state must be equal, i.e.

$$\begin{aligned} u_0^1 = u_0^2 = u_0^3, \;\; u_1^1 = u_1^2 = u_1^3, \\ u_1^4 = u_1^5 = u_1^6, \;\; u_1^7 = u_1^8 = u_1^9 \end{aligned}$$

Hence, the future inputs are allowed to change in accordance with new information received through feedback. This increases the flexibility of the NMPC and reduces the conservativeness (Lucia et al., 2013).

The robustified NMPC from Ersdal et al. (2016b) is from now on referred to as the multi-stage NMPC (MNMPC), and it is a multi-stage NMPC where three disturbance realizations are considered; one following the positive border of $\mathcal{W}$, one following the negative border of $\mathcal{W}$, and one neutral in the middle. Compared to the scenario tree in Fig. 1, this means that three paths are included: $w^1 = \{w_0^1, w_1^1, w_2^1, \ldots\}$, $w^2 = \{w_0^2, w_1^2, w_2^2, \ldots\}$, and $w^3 = \{w_0^3, w_1^3, w_2^3, \ldots\}$. These corresponds to w^p, w^z, and w^n in Fig. 2. In accordance to Lucia et al. (2013), the first element of u must be equal for all three scenarios ($u_0^p = u_0^z = u_0^n$), after this, they are free to vary in manners optimal for their designated system states, see Fig. 2.

The OCP solved at each time instant in the MNMPC is then

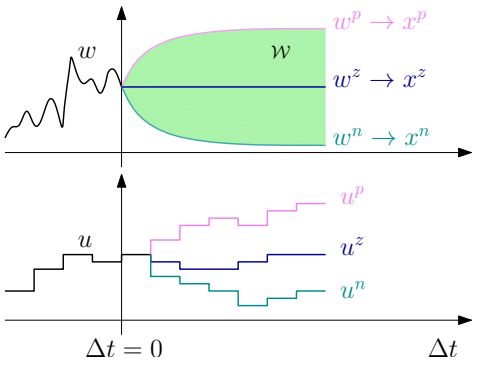

Fig. 2. Sketch of how the MNMPC works. For simplicity of illustration, u is considered to be scalar.

$$\min_{u^j \forall j} \sum_{j=\{p,z,n\}} J\left(x^j, u^j\right) \tag{8a}$$

$$\dot{x}^j - f\left(x^j, u^j, w^j\right) = 0 \quad \text{System model} \tag{8b}$$

$$\left.\begin{array}{l} g\left(x^j, u^j\right) \leq 0 \\ u_0^z = u_0^p = u_0^n \end{array}\right\} \text{ Constraints} \tag{8c}$$

where $j = \{p, z, n\}$, x^j, w^j, u^j the state, disturbance and input associated with scenario j, and $J(x^j, u^j)$ the following objective function.

$$J\left(x^j, u^j\right) = \int_{t=0}^{T} x^{jT} Q^j x^j + u^{jT} R^j u^j \;\; dt \tag{9}$$

4. CASE STUDY

The SNMPC is tested on the SINTEF Nordic power system test bed from Ersdal et al. (2016b) and compared against the MNMPC. The PM in Section 2 is chosen to have 2 areas, hence $N = 2$. One area covers South Sweden and Eastern Denmark (area A), and the other covers Norway, North Sweden and Finland (area B), and according to the assumptions made in Section 2, $\Delta P_D^B = 0$ and $\Delta P_D = \Delta P_D^A$. There is also a tie line between the two areas which represents the total power flow between them, and has a positive direction from area B to area A. The extended Kalman filter (EKF) presented in Ersdal et al. (2016b) is also applied here to close the control loop. The proxy system and both NMPCs were implemented in Python using Casadi, where the continuous time OCPs (5) and (8) are discretized and transformed into nonlinear programs. Collocation has been used for discretization, and the OCPs are solved using the interior point optimizer IPOPT (Wächter and Biegler, 2006).

The SNMPC-OCP (8) has 32 optimization variables n_u, and in order to obtain acceptable probability results in (7), the number of scenarios should approach $S = 1000$. With the hardware and software used in this work, such a large number of scenarios imposes computer memory issues that are difficult to handle. Computational issues when implementing stochastic NMPC are not unexpected. In Rostampour et al. (2015), for example, it takes more than 5 days to solve the OCP with $S = 100$, while the sampling time of the NMPC is 15 s. We therefore limited us to $S = 65$. It is seen through simulations that the behavior of the SNMPC in the test case does not change much from $S = 10$ to $S = 65$, and so it is assumed that for the purpose of comparison with the MNMPC, the simulation

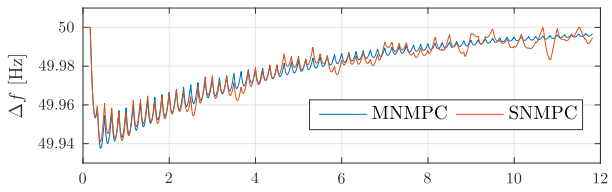

Fig. 3. Case A: Frequency deviation for MNMPC and SNMPC.

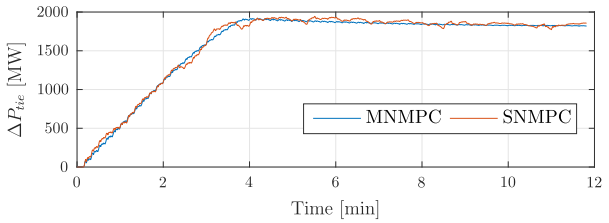

Fig. 4. Case A: Tie-line power flow for MNMPC and SNMPC.

results from $S = 65$ can be used as a representation of a stochastic NMPC scheme with more realistic values for β and ϵ.

In order to compare the two controllers, a control performance measure (CPM) is applied, which is calculated in the following manner: First, Δf is averaged over windows of 30 s to filter out fast fluctuations. Second, the CPM is found by again averaging Δf over all these windows. This CPM is inspired by the CPS1 and CPS2 performance criteria used by the North American electric reliability corporation (NERC) (Gross and Lee, 2001).

4.1 Tuning the NMPC

The main tuning variables for the NMPCs are the prediction horizon T and the objective function $J(\cdot)$. The objective function for both the SNMPC and the MNMPC is set to

$$J\left(x^j, u^j\right) = \int_{t=0}^{T} x^{jT} Q^j x^j + u^{jT} R^j u^j \; dt \qquad (10)$$

For both the SNMPC and the MNMPC, Q is real, symmetric and positive semidefinite, while R is real, symmetric and positive definite. The non-zero elements of Q are chosen so that the deviation in overall system frequency is punished Ersdal et al. (2016b): $q_{11} = \gamma \frac{\left(H^1\right)^2}{(H^1+H^2)^2}$, $q_{66} = \gamma \frac{\left(H^2\right)^2}{(H^1+H^2)^2}$, $q_{16} = q_{61} = \gamma \frac{H^1 H^2}{(H^1+H^2)^2}$, where $\gamma = 10^5$. The matrix R is set to $R = \text{diag}\left(\eta m_{\text{base}}\right)$, where m_{base} is a vector containing the hydro generators' base rating, and $\eta = 0.1$. For the MNMPC $Q^p = Q^n = 0.1Q^z$ in order to place more emphasis on deviations in x^z. The three systems are all punished equally when it comes to deviations in input: $R^z = R^p = R^n$. For the SNMPC all scenarios have the same Q and R.

The control horizon T is 3 minutes for both NMPCs, a decision based on a compromise between system time constants and complexity, and the time step of the NMPCs is 10 s in order to match the control signal dispatching in the system.

4.2 Simulation results

Case A Both the SNMPC and the MNMPC are simulated with a disturbance $w = w_n$, see Fig. 2, and a maximum transfer limit from area B to area A at $\Delta P_{tie,max} = 2000$ MW. The resulting Δf and ΔP_{tie} can be seen in Fig. 3 and 4. They show that the resulting frequency deviation and tie-line power flow are very similar in the two cases. Both controllers bring the frequency back to 50 Hz while keeping a clearance to the tie-line limit of 2000 MW in case of new disturbances. This is supported by the CPM given in Table 2. It is assumed that the similarity in behavior will increase concurrently with S, which makes sense as w^p and w^n define the boundaries for $\mathcal{W}$ and hence for the scenarios w^j. When the number of scenarios S is increased, so will the scenario's coverage of $\mathcal{W}$, resulting in a SNMPC which must take into account disturbance scenarios similar to w^n and w^p. The SNMPC will also naturally place more emphasis on the average disturbance scenario through a higher scenario density near the center of $\mathcal{W}$, while the MNMPC does the same by applying a higher weight to Q^n in the objective function.

Table 2. CPM and average optimization time T_{opt} for Case A.

Controller	CPM $\left(\cdot 10^{-5}\right)$	T_{opt}
Multi-stage	11.18	1.98 s
Stochastic	11.23	40.18 s
Difference	+0.5%	+1910%

However, as seen in Fig. 3 and 4, the SNMPC results in a more "noisy" system behavior than the MNMPC. There are two main reasons for this. First of all, the scenarios used in the SNMPC fluctuate more than the smooth disturbance scenarios used in the MNMPC. These high frequency fluctuations will excite the fast system dynamics in the predictions, resulting in a more fluctuating and conservative controller. Secondly, the fact that the SNMPC has one common optimized input for all scenarios forces the input to fluctuate in order to fulfill system constraints for all scenarios, which again excites the dynamics of the actual system.

Case B In Case B the transfer capacity on the tie line is changed so that the transfer window is more narrow than in Case A. The limits are now set to $\Delta P_{tie,min} = -100$ MW and $\Delta P_{tie,max} = 1000$ MW, resulting in a transfer window of 1100 MW. Fig. 5 shows the predictions associated with w^p and w^n from the MNMPC-optimization at $t = 0$, and Fig. 6 shows the predictions associated with two of the disturbance realizations from the last attempt at solving the SNMPC-optimization at $t = 0$.

In this case, the SNMPC was not able to find a feasible solution, and the reason for this is illustrated in Fig. 6. It shows that the SNMPC is simply not able to find a common input which fulfills the system constraints for all disturbance scenarios over the entire prediction horizon. Up until approximately 2.5 minutes into the prediction horizon, the tie-line power transfer associated with w^{31} and w^{40} are kept at, or within, the transfer limits by keeping the total input relatively low. After this, however, it seems that some adjustments are to made, and the input

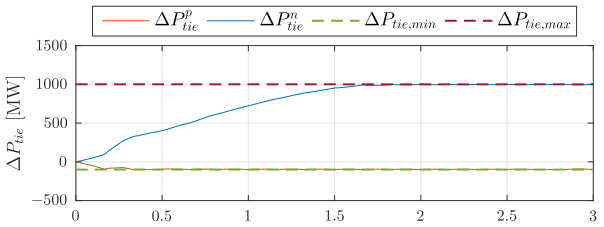

(a) Predicted tie-line power flow associated with w^p and w^n.

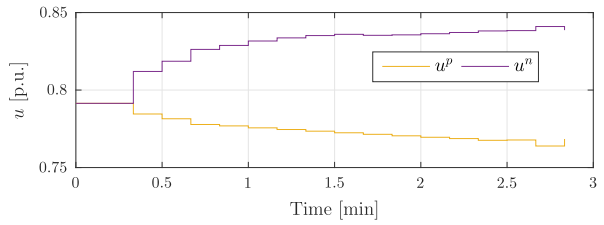

(b) Sum of predicted input associated with w^p and w^n.

Fig. 5. Case B MNMPC: Predicted input and tie-line power flow.

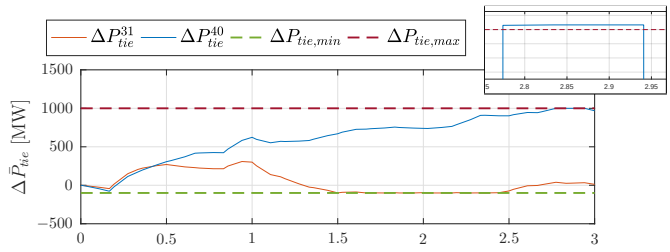

(a) Predicted tie-line power flow associated with w^{31} and w^{40}.

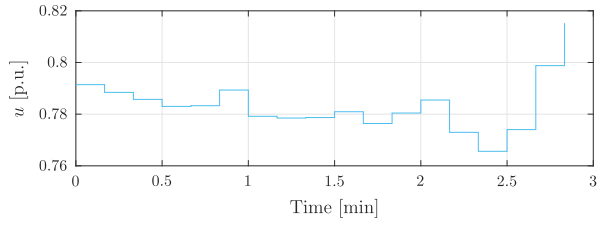

(b) Sum of predicted input for both w^{31} and w^{40}.

Fig. 6. Case B SNMPC: Predicted input and tie-line power flow. A zoomed picture showing that ΔP^{40}_{tie} violates the upper limit.

is increased, likely as an effort to keep ΔP^{31}_{tie} within the lower transfer limit. This in turn causes ΔP^{40}_{tie} to increase, and violate the upper transfer limit, as seen in the zoomed square of Fig. 6(a).

The MNMPC is on the other hand able to find a feasible solution, and even though both ΔP^p_{tie} and ΔP^n_{tie} stay at the limits, they never violate them. Fig. 5(b) shows how the inputs associated with w^p and w^n are free to vary after the first time steps, and this is the reason why the MNMPC is able to find a feasible solution while the SNMPC is not.

4.3 Discussion

The benefit of the SNMPC is clearly the stochastic guarantees for constraint fulfillment given by Theorem 1 in Campi et al. (2009). With $S \approx 1000$, it would be guaranteed that with no probability smaller than 0.99, u^* would satisfy all system constraints for all $w \in \mathcal{W}$ except for a small fraction of them whose probability is smaller than or equal to 0.07. These are theoretical guarantees which cannot be made for the MNMPC. They are however made under unrealistic assumptions such as perfect prediction model, and the practical implications are therefore arguable. It is the authors' opinion that the constraints of the control problem presented in this paper are of such a nature that the practical difference with respect to constraint fulfillment is not prominent. However, it should be mentioned that the SNMPC does have the advantage of freedom to tune the conservativeness through the choice of η and β (and hence S), which is not as easy for the MNMPC.

There are also some issues with the tractability of the SNMPC as S increases. The MNMPC considers much fewer scenarios than the SNMPC, and therefore solves a much smaller OCP. This is reflected in the maximum optimization time in Case A, which was 2.1 s and 59.8 s for the MNMPC and the SNMPC, respectively, with an average optimization time of 2.0 s and 40.2 s. If a successful simulation of SNMPC with $S = 1000$ could be conducted, the optimization time would increase even further, and with a time step of 10 s, this means that the MNMPC is able to run in real time, whereas the SNMPC is not. It can be argued that some of these tractability issues can be resolved using more memory etc., however, the MNMPC will still solve the OCP in less time.

Another issue is the feasibility and recursive feasibility of the OCP. For both the MNMPC and the SNMPC there are no guarantees for neither feasibility nor recursive feasibility. However, in the MNMPC the optimization variable u for each disturbance realization $\{w^z, w^p, w^n\}$ only needs to be equal for the first instant, before they are free to do what is optimal for their associated system states $\{x^z, x^p, x^n\}$, whereas for the SNMPC u is equal for all disturbance realizations and their associated system states. This complicates matters for the SNMPC with regards to feasibility, as seen in Case B. When the scenarios included in the SNMPC results in diverging system behavior and thereby diverging inputs needs, it becomes increasingly difficult as S increases to find one common input to satisfy them all. It could be argued that feedback could be included in the SNMPC as well, this would however increase the already prominent tractability issues. If each of the scenarios of the SNMPC were to have their own input, the size of the OCP would increase substantially. In addition, since Theorem 1 from Campi et al. (2009) is developed with one common input for all scenarios, it may not hold if feedback was included. When it comes to recursive feasibility, the MNMPC results in a standard, nominal NMPC, and recursive feasibility can be guaranteed using classical methods such as terminal constraint regions which are control invariant (Maiworm et al., 2015), provided that such terminal ingredients can be calculated a priori. In the general nonlinear case it is however very challenging to find the necessary terminal ingredients, and if they can be found, they often lead to overly conservative control laws (Lucia et al., 2014a).

An important strength of the SNMPC is the fact that the number of scenarios S necessary to achieve probabilistic guarantees, is independent of the number of uncertainties

included in the problem. This means that if the uncertainty of produced wind power would enter the power system in more than one area, the number of S would not increase. The only thing that would change is the way these S scenarios are generated. With the MNMPC however, the scenario tree would include many more scenarios, and finding the worst case disturbance scenario would be much more difficult. In this work, there is only one disturbance acting on the system, so this feature of the SNMPC is not displayed.

The MNMPC and the SNMPC are based upon two different disturbance modeling paradigms; deterministic and stochastic. And even though it could be argued that it is intuitive to view the future variation from the predicted wind-power production as stochastic, the robust control issue in this paper is mainly handling the worst case disturbance, since handling of the worst-case disturbance implies that less severe disturbances can be handled as well. The case study presented in this paper illustrates that the SNMPC and the MNMPC have some similarities in practice, however, the MNMPC is less conservative and less likely to encounter feasibility issues because it takes into account feedback in its predictions.

5. CONCLUSION

This paper presents a stochastic NMPC (SNMPC) for frequency control of the Nordic power system, and compares it with the multi-stage NMPC (MNMPC) presented in Ersdal et al. (2016b). The nonlinearities of the SNMPC are very modest, and the theory on stochastic assurance of constraint fulfillment from Campi et al. (2009) is used as if the optimal control problem of the SNMPC was convex.

Simulations on a proxy of the Nordic power system show that the SNMPC and the MNMPC behaves similarly, and it argued that the SNMPC and the MNMPC share some properties in practice. However, the MNMPC does not give stochastic guarantees for constraint fulfillment, such as the SNMPC. The practical consequences of this are unclear, especially given that these guarantees do not take into account other unknown disturbances and model errors. On the other hand, the MNMPC is less likely to encounter infeasibility, and there are also tractability and real-time issues with the SNMPC which are not seen in the MNMPC.

REFERENCES

Barry, R. and Chorley, R. (2003). *Atmosphere, Weather, and Climate*. Routledge.

Bemporad, A., Borrelli, F., and Morari, M. (2003). Min-max control of constrained uncertain discrete-time linear systems. *Automatic Control, IEEE Transactions on*, 48(9), 1600–1606.

Bemporad, A. and Morari, M. (1999). Robust model predictive control: A survey. *Robustness in identification and control*, 207–226.

Campi, M.C., Garatti, S., and Prandini, M. (2009). The scenario approach for systems and control design. *Annual Reviews in Control*, 33(2), 149–157.

Cecílio, I.M., Ersdal, A.M., Fabozzi, D., and Thornhill, N.F. (2013). An open-source educational toolbox for power system frequency control tuning and optimization. In *Innovative Smart Grid Technologies Europe (ISGT EUROPE), 2013 4th IEEE/PES*. IEEE.

Ersdal, A., Imsland, L., and Uhlen, K. (2016a). Model predictive load-frequency control. *Power Systems, IEEE Transactions on*, 31(1), 777–785.

Ersdal, A.M., Imsland, L., Uhlen, K., Fabozzi, D., and Thornhill, N.F. (2016b). Model predictive load–frequency control taking into account imbalance uncertainty. *Control Engineering Practice*, 53, 139–150.

Gross, G. and Lee, J.W. (2001). Analysis of load frequency control performance assessment criteria. *Power Systems, IEEE Transactions on*, 16, 520–525.

Holttinen, H. (2004). *The impact of large scale wind power production on the Nordic electricity system*. Ph.D. thesis, Helsinki University of Technology.

Langson, W., Chryssochoos, I., Raković, S., and Mayne, D. (2004). Robust model predictive control using tubes. *Automatica*, 40(1), 125 – 133.

Levine, W. (2010). *The Control Handbook, Second Edition: Control System Fundamentals*. Electrical Engineering Handbook. CRC Press.

Li, P., Wendt, M., and Wozny, G. (2002). A probabilistically constrained model predictive controller. *Automatica*, 38(7), 1171–1176.

Lucia, S., Limon, D., and Engell, S. (2014a). Stability properties of multi-stage robust nonlinear model predictive control. *Automatica (Submitted)*.

Lucia, S., Andersson, J.A., Brandt, H., Diehl, M., and Engell, S. (2014b). Handling uncertainty in economic nonlinear model predictive control: A comparative case study. *Journal of Process Control*, 24(8), 1247–1259.

Lucia, S., Finkler, T., and Engell, S. (2013). Multi-stage nonlinear model predictive control applied to a semi-batch polymerization reactor under uncertainty. *Journal of Process Control*, 23(9), 1306 – 1319.

Maciejowski, J.M. (2002). *Predictive Control with Constraints*. Pearson Education.

Maiworm, M., Bäthge, T., and Findeisen, R. (2015). Scenario-based model predictive control: Recursive feasibility and stability. *The 9th IFAC Symposium on Advanced Control of Chemical Processes ADCHEM 2015*, 48(8), 50 – 56.

Mesbah, A. (2016). Stochastic model predictive control: An overview and perspectives for future research. *IEEE Control Systems*, 36(6), 30–44.

Primbs, J.A. and Sung, C.H. (2009). Stochastic receding horizon control of constrained linear systems with state and control multiplicative noise. *Automatic Control, IEEE Transactions on*, 54(2), 221–230.

Rawlings, J.B. and Mayne, D.Q. (2009). *Model Predictive Control: Theory and Design*. Nob Hill Publishing.

Rostampour, V., Esfahani, P.M., and Keviczky, T. (2015). Stochastic Nonlinear Model Predictive Control of an Uncertain Batch Polymerization Reactor. In *IFAC Conference on Nonlinear Model Predictive Control*.

Rostampour, V., Margellos, K., Vrakopoulou, M., Prandini, M., Andersson, G., and Lygeros, J. (2013). Reserve requirements in ac power systems with uncertain generation. In *IEEE PES ISGT Europe 2013*, 1–5.

Scokaert, P. and Mayne, D. (1998). Min-max feedback model predictive control for constrained linear systems. *IEEE Transactions on Automatic Control*, 43(8), 1136–1142.

Shiroei, M., Toulabi, M.R., and Ranjbar, A.M. (2013). Robust multivariable predictive based load frequency control considering generation rate constraint. *International Journal of Electrical Power & Energy Systems*, 46, 405–413.

Statnett (2012). Systemdrifts- og markedsutviklingsplan 2012. Technical report. Available at `issuu.com/statnett/docs/statnett_smup`.

Venkat, A., Hiskens, I., Rawlings, J., and Wright, S. (2008). Distributed mpc strategies with application to power system automatic generation control. *Control Systems Technology, IEEE Transactions on*, 16(6), 1192–1206.

Wächter, A. and Biegler, L.T. (2006). On the implementation of an interior-point filter line-search algorithm for large-scale nonlinear programming. *Mathematical Programming*, 106(1), 25–57.